

SEMIANNUAL STATUS REPORT

FOR PERIOD 1 JULY 1965 THROUGH 31 DECEMBER 1965

Required under the terms of NASA Research Grant Nsg 443

"Research Related to an Experimental Test of General Relativity"


Under the Direction of
H. W. Knoebel and W. D. Compton

FACILITY FORM 802	N67-81188	
	(ACCESSION NUMBER)	(THRU)
	16	None
	(PAGES)	(CODE)
	CIR 70258	
	(NASA CR OR TMX OR AD NUMBER)	(CATEGORY)

COORDINATED SCIENCE LABORATORY

University of Illinois
Urbana, Illinois

January 1966



Gyro Electrical Conductivity

An acceptable range of electrical conductivity for the gyro material has been determined from the following considerations. In order to avoid drift torque due to localized charge on a sphere in an electric field the charge must be uniformly distributed with a relaxation time τ less than one gyro revolution. From the relation

$$\tau = \rho_e \epsilon$$


where ρ_e is the electrical resistivity and ϵ is the dielectric constant, an upper bound of 10^{10} ohm cm is obtained for the electrical resistivity for our gyro parameters. The lower bound is obtained from the drift torque due to eddy currents flowing on the gyro spinning in the earth's magnetic field. From the relation

$$\dot{\phi} = \frac{B^2}{8\rho_e \rho_m} \times 10^{-9}$$

where $\dot{\phi}$ is the gyro spin axis precession in radians/sec, B is the earth's magnetic field in gauss, ρ_e is the electrical resistivity in ohm cm and ρ_m is the mass density in gm/cm³, a value of $\rho_e = 1.6 \times 10^3$ ohm cm is obtained as the lower limit for a maximum $\dot{\phi}$ of 0.6 arc sec/year, for $B = 1/2$ gauss and $\rho_m = 2.5$ gm/cm³. Hence, the range of electrical resistivity has been established as approximately

$$2 \times 10^3 \leq \rho \leq 10^{10} \text{ ohm cm.}$$

A conservative calculation for a sphere spinning in an electric field in which induced charges slide along the resistive spherical surface as the sphere rotates shows that a negligible drift torque exists for the worst case of $\rho = 10^{10}$ ohm cm. Materials with resistivities in the established range are being investigated.



Influence of Meteoroids

The degree to which the relativity satellite of the Coordinated Science Laboratory is immune to the momentum transfer of impacting meteoroids depends upon the model of the meteoroid flux. The best known, and also the most conservative model of the meteoroid environment was developed by Whipple in 1957. This model can be represented by

$$\phi_1 = 1.3 \times 10^{-12} m^{-1} \quad (1)$$

where ϕ is the flux/meter² sec of particles with mass m grams and greater.¹ A 1961 evaluation of rocket and satellite data obtained

$$\phi_2 = 10^{-17.0} m^{-1.70}, \quad (2)$$

applicable between masses of 10^{-10} to 10^{-6} gm.¹ However, observations of meteors simulated by shaped charge firings indicated that Whipple's 1957 estimate should be revised by an order of magnitude to give¹

$$\phi_3 = 1.3 \times 10^{-13} m^{-1} \quad (3)$$

These are three meteoroid models currently used, all subject to revision as more is learned of the space environment.

The number of particles hitting a given satellite in a given amount of time can be calculated using the flux expression to be

$$N = \phi AT$$

where A is the area exposed to meteoroids and T is the time of exposure.

¹Orbital Flight Handbook, NASA Sp 33, Part 1, pp II46-II47.

Assume, for calculation purposes, a possible CSL gyro satellite to be a solid, nearly spherical body of density 2.2 gm/cm^3 , having a radius of 15 cm, spinning at 250 rev/sec and monitored for one year. A plot of the number of meteoroids striking the satellite versus the meteoroid mass is given in Fig. 1 using the above satellite radius and the three different flux estimates. Figure 1 reveals that large numbers of small meteoroids will hit the satellite while few meteoroids heavier than 10^{-5} grams are to be expected within a year's time.

The effect of a meteoroid hit will depend upon the momentum of the impinging particle. Visual observations of meteor showers indicate that large meteoroids have approximate velocities of 28 km/sec while smaller particles have a velocity of about 15 km/sec. The velocity distribution tabulated in table 35 of ref. 1 is used for calculations in this analysis. A conservative approach to the momentum exchange analysis is to assume that the momentum vector of all impinging particles is perpendicular to the spin axis and passes through the spin axis. The impulsive angular displacement, δ , caused by one meteoroid hit would then be

$$\delta = \frac{mvr}{C\Omega}$$

where C is the moment of inertia, Ω is the spin rate, and mv is the momentum of the meteoroid acting at a distance r from the center of mass of the satellite. For a conservative calculation let r be the radius of the satellite, R . The moment of inertia of the spherical gyro is

$$C = \frac{8}{15} \rho_s R^5$$

where ρ_s is the density, and the impulsive angular deviation due to one meteoroid hit becomes

$$\delta = \frac{15}{8\pi} \frac{mv}{\rho_s R^4 \Omega} \quad . \quad (4)$$

A large satellite then would be less affected by meteoroid hits than a smaller one. However, a larger satellite is hit by a greater number of particles. This can be taken into consideration by assuming a mean square deviation of events along the spin axis and writing an expression for the net angular deviation, σ , of N hits,

$$\sigma = \delta \sqrt{N} \quad .$$

This function is plotted versus meteoroid mass in Fig. 2 using the conservative 1957 Whipple estimate of meteoroid flux. Since the surface area of a sphere is $4\pi R^2$, σ is inversely proportional to the radius cubed.

Figure 2 indicates that the larger meteoroids will be detrimental to the relativity experiment which requires spurious deviations of less than 1 sec of arc per year. However, the probability of being hit by the larger meteoroids is of course less than for the smaller particles. Assuming a Poisson distribution of events the probability of no impact, $P(0)$, within a year by a meteoroid of a given mass is given by

$$P(0) = e^{-N}$$

where $N = \phi AT$. Therefore, for a meteoroid of a given mass, the maximum impulsive precession due to its impact and the probability of it not hitting the satellite can be calculated. A plot of $P(0)$ versus δ using

the three meteoroid flux models is given in Fig. 3. This plot can be interpreted to give the probability of success of the experiment with reference to meteoroids if a maximum δ to be tolerated is defined. For the CSL Relativity experiment this maximum δ would be 1 sec of arc in a year which would correspond to better than 97% chance of success using the most conservative flux estimate. The effect of meteor showers in which the flux rate may increase by two or three orders of magnitude is being investigated.

Gyro Diameter Optimization

The previous report analyzed the gyro torque due to gravity gradient for a non-regressing orbit. The present report extends this analysis for a regressing orbit due to the earth's oblateness. Furthermore, the effects of centrifugal deformation and the statistics of micrometeorite cratering along with the effects of gravity gradient give rise to an optimum gyro diameter, as shown by the following discussion.

The spin axis deviation due to gravity gradient for a gyro orbiting in a regressing, elliptic orbit is

$$\dot{\phi} = -2Kg [\sin i \cot \epsilon \cos (\Omega - \phi) - \cos i] \cos \theta \quad (5)$$

$$\dot{\epsilon} = -2Kg \sin i \sin (\Omega - \phi) \cos \theta \quad (6)$$

where

i is the orbital inclination

Ω is the right ascension of the orbit

ϵ is the inclination of the gyro equatorial plane

ϕ is the right ascension of the gyro

θ is the angle between the gyro spin axis and the orbital plane

$$\text{and } K_g = \frac{3}{4} \frac{GM}{a^3 \omega_s} \frac{(1 + \frac{3}{4} e^2)}{(1 - e^2)^3} \left(\frac{C-A}{C} \right) \quad (7)$$

where

G is the universal gravitational constant

M is the mass of the earth

a is the semi-major axis of the orbital ellipse

e is the eccentricity of the ellipse

ω_s is the gyro angular velocity

C is the gyro polar moment of inertia

A is the gyro transverse moment of inertia.

Because of centrifugal deformation the gyro moment of inertia ratio $\frac{C-A}{C}$ can be written as the sum of two components — a static or manufactured component $(\frac{C-A}{C})_s$ and a component due to centrifugal deformation, so that

$$\frac{C-A}{C} = \left(\frac{C-A}{C} \right)_s + \frac{F(\sigma) \rho r^2 \omega^2}{E} \quad (8)$$

where

$F(\sigma)$ is a function of the Poisson ratio

ρ is the gyro density

E is the modulus of elasticity

r is the gyro radius.

A plot of K_g versus r for various peripheral velocities $v = \omega r$ from equation (7) is shown in Fig. 4. Orbital eccentricities smaller than 0.1 are used, in which case the error in K_g is less than 4 percent. From a family of such plots it is found that the values of r and v which produce the minimum value of K_g also cause the centrifugal deformation inertia ratio component to equal the static value component. It is also

seen from Fig. 4 that the curve of K_g vs r has a broad minimum which includes the reasonable gyro radius of 15 cm. From Eqs. (7), (8), and Fig. 4, it can be shown that for minimum K_g , and hence minimum precession, the peripheral velocity v should be as large as possible and the static inertia ratio be as small as possible. For most materials the yield point is reached when the peripheral velocity is about 300 meters/sec.

The data readout system requires a finite $(\frac{C-A}{C})_s$. This is seen from Fig. 4 of the previous status report, in which the number of hits per year, each of which could cause an angular disturbance of 0.6 arc sec, is plotted versus $\frac{C-A}{C}$. For this plot the meteoroid flux model of Eq. 3 was used. If such disturbances occur at a rate less than once per month and for a spin axis damping time of less than one day the effect of the disturbance can be readily removed from gyro spin axis orientation data. Assuming the meteorite flux has a Poisson distribution, then if angular disturbances of one-tenth the relativity effect occur once per year, the probability of having one month of undisturbed data is 0.92 and, from Fig. 4 of the previous status report the required $\frac{C-A}{C}$ ratio is 0.01. The curves for this figure are for a 15 cm radius solid. For a fused silica gyro of 15 cm radius and a peripheral velocity of 300 meter/sec, K_g is about 40 arc sec per year.

From Eqs. (1) and (2), the theoretically determined minimum value of K_g and the requirement that the spurious gyro drift be one order of magnitude less than the general relativity precession the requirements are obtained that the gyro spin axis must lie in the plane of either a polar orbit or the earth's equatorial plane for a nearly equatorial orbit to better than 0.44 degrees.

Photographic Observability

On a recent visit to the Smithsonian Astrophysical Observatory, it was learned that the observable energy flux for the Baker-Nunn camera is approximately 8×10^{-11} lumen second per square meter. This was quoted as producing a reliably observable image of a point source in competition with a one-second exposure to night sky, in that the night sky produces a photographic density 0.3 to 0.4 logarithmic density unit below the density produced by the point source. The energy flux is quoted for the input to the camera aperture, for a spectral distribution corresponding to the solar color temperature, as seen through the earth's atmosphere, and using red-extended Royal-X Pan film for reciprocity conditions favoring fractional-second exposure times.

This "threshold" corresponds to observing a solar flash near the zenith from a mirror facet of 60 square centimeters in projected area, at a range of 1000 kilometers, and for a flash duration of 7 microseconds. The duration is the time required for the satellite to rotate through 0.25 degree at a rotation rate of 100 Hz, to scan the half-degree width of the solar image. At this slant range, the orbital speed would correspond to an apparent speed of 0.4 degrees per second. At a flash rate of 500 Hz, the apparent flash spacing would be about three seconds of arc. Thus, within the optical resolution of the camera, some 12 seconds of arc, there would fall four flashes, producing an exposure above "threshold" by a factor 4. Actually observed resolutions involve some image spreading, resulting from light scatter within the film, so that a factor of 6 could be claimed. The method of data detection and analysis to be used, however, will involve correlation techniques exploiting the total energy in the flash pattern, involving some 400

flashes, so that the effective total exposure above "threshold" would be, allowing for the fact that not all flashes would be at the maximum intensity, nearer a factor of 200.

The detection and analysis of the flash pattern for an optical determination of the center of the pattern will require correlation of the observed pattern with one derived from the pattern to be expected a priori. The derivation would reflect the nonlinearity of the photographic film together with a knowledge of the noise statistics of the film. For example, if the film were linear, and the noise statistics were gaussian with signal-independent parameters, then the optimal pattern would be the angular derivative of the expected brightness pattern, for the estimation of the pattern center.

It will then be important to develop accurate models of the photographic linearity and noise parameters in order to develop the estimation pattern for use in the correlation technique, and also, through computer simulations, to develop firm estimates of the accuracy that may be expected. Experimental work to this end will be started soon.

At the present time, however, a reliable accuracy estimation cannot be obtained, based on signal-to-noise considerations. It is not realistic, for example, to regard the Baker-Nunn "threshold", cited above, as equivalent to a noise level against which the optical brightness should be compared, in any literal sense. The density increment of 0.3 to 0.4 does correspond to a light transmission ratio of from a factor 2 to 2.5, but one does not know from this that the single-flash exposure, as described, is above the background by so small a factor. Typically, the density-vs-log-exposure curve would have a slope near 0.3 for exposures near the toe of the curve, so that the exposure ratio, corresponding to a density difference of 0.3, could be nearer the factor 10.

Questions relating to the noise level must also involve an estimate of the noise bandwidth, related to that needed to accommodate the signal. This noise arises from the random granularity of the photographic image. It was observed that a "point" image from the Baker-Nunn camera would be 10 or so grains wide, suggesting a bandwidth ratio of 10. Thus, a microdensitometer tracing using a very small aperture would show 10 times as much noise energy as a tracing using an aperture matched to a resolution width. The description of the "threshold" image as being "reliably observable" would be unusual for a signal presented at a signal-to-noise ratio of 2, for which the noise bandwidth matched that of the signal, but would be an eminently reasonable description at a signal-to-noise ratio of 10.

With some hope of realism, one could then estimate the "threshold" point-image signal-to-noise ratio as being of the order of 10, or even more if referred to exposure. In the same way, one could estimate the integrated whole-pattern signal-to-noise ratio to be 2000 or more, under the cited circumstances, with more reliable estimates to be obtainable after more study. Using these considerations, the accuracy for measuring the position of extended images should be estimated to be consistent with that usually quoted for the Baker-Nunn camera, namely 2 seconds of arc for laboratory measurements.

It will be noted that the number of flashes that will fall in a resolution element will increase with range, but that the brightness of each flash will decrease with the square of the range, so that the photographic effect will decrease with the first power of range, in a manner characteristic of line sources.

The sensitivity to other parameter variations is less severe. For example, a decrease in rotation rate will increase the exposure for each flash, but decrease the number within a resolution element, so that the net exposure would be the same. Similarly, an increase in the area of the facets, at the expense of reducing the number contributing to a given pattern, will result in no change in observability.

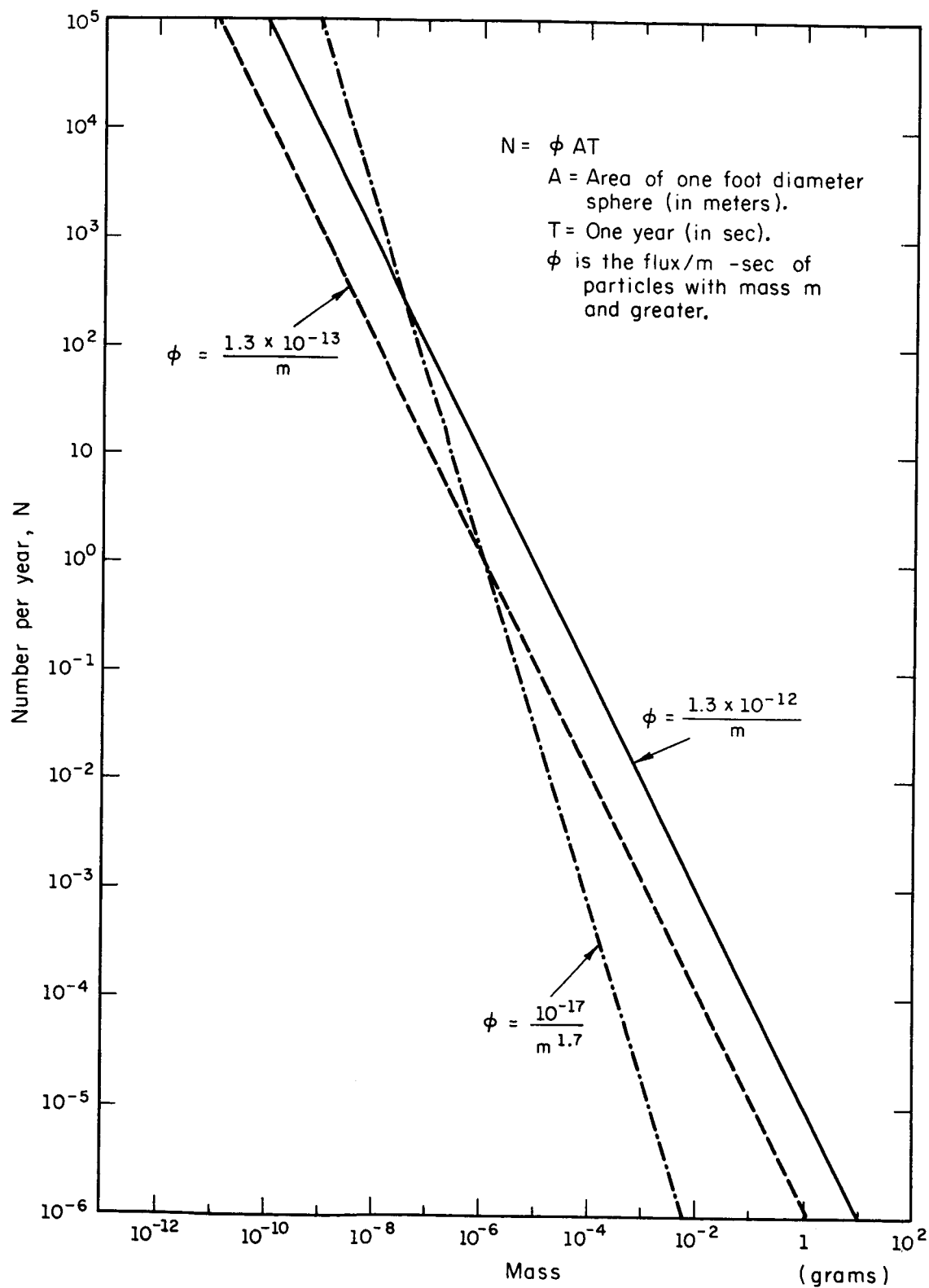


Fig. 1. Number of meteoroids striking proposed gyro per year versus the meteoroid mass for three flux models.

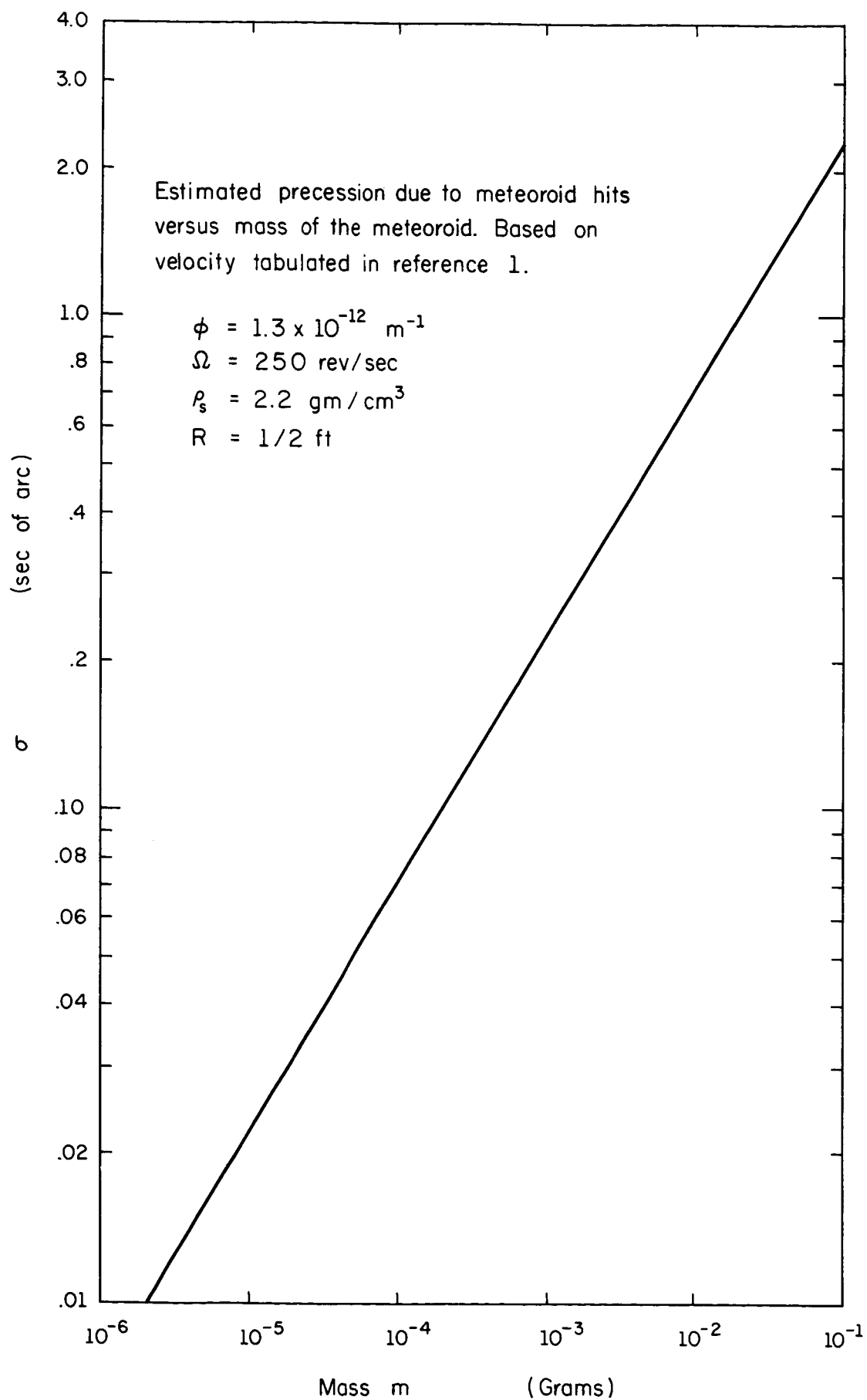


Fig. 2. Net angular deviation of gyro spin axis versus meteoroid mass.

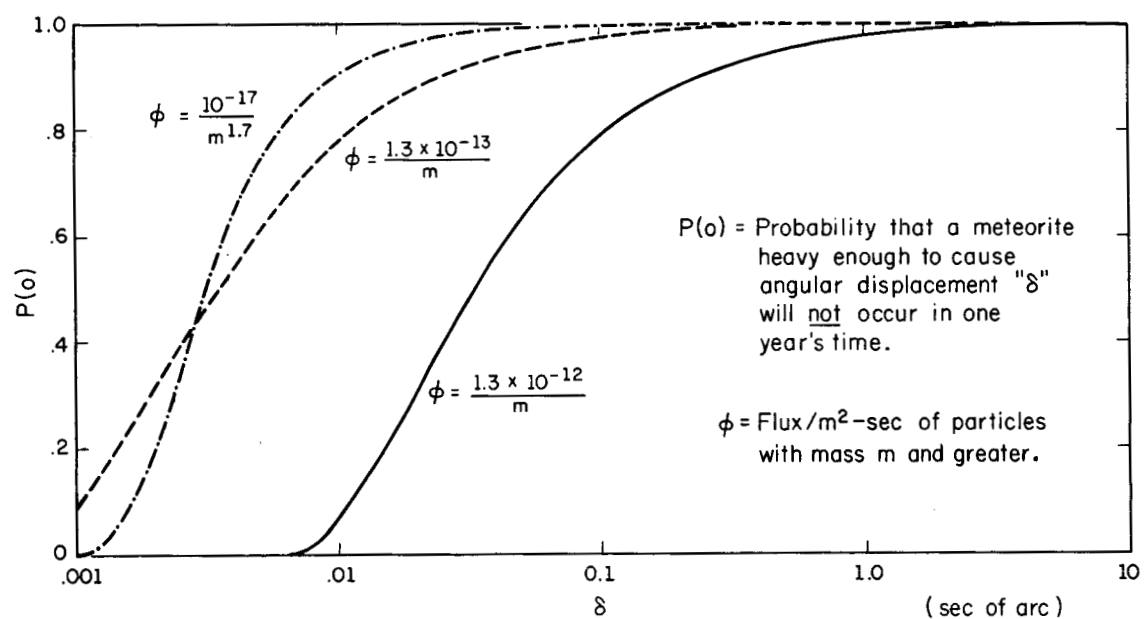


Fig. 3. Probability of no meteoroid impact with the proposed gyro in one year versus the impulsive angular deviation due to one impact, for three flux models.

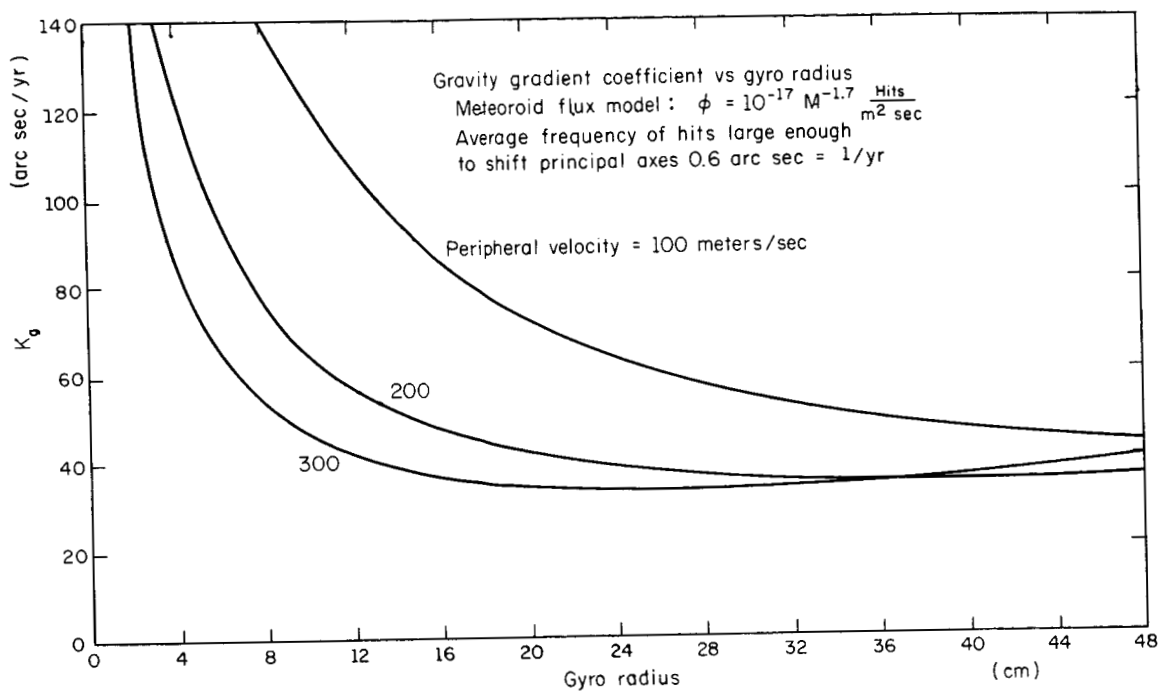


Fig. 4. K_g versus Gyro Diameter r for Various Peripheral Velocities.